Chemical Fuel-Driven Stiffening of Transient Hydrogels via Vitrifiable Phase Separation

Ying Zhao, Baohu Wu, Shengtong Sun, and Peiyi Wu**

Abstract: Fuel-driven transient materials that can temporally adjust their mechanical properties are ubiquitous in living systems, enabling biological functions to be maintained far from equilibrium. While numerous biomimetic transiently stiffened materials have been developed, their low stiffened moduli (typically in the kPa range) severely restrict their practical use in load-bearing applications. Here we report a chemically fueled transient hydrogel that can stiffen into a highly rigid glassy state via vitrifiable bicontinuous phase separation. The hydrogel is made from thermal-stiffening poly(zinc acrylate)-based copolymers, with the stiffening temperature being precisely regulated by the acrylic acid content. Carbodiimide triggers the temporary conversion of carboxylic acids to hydrophobic anhydrides, drastically lowering stiffening temperature and vitrifying polymer-rich phase under ambient conditions. Consequently, the initial soft hydrogel transforms into a transient glassy state, achieving an ultrahigh modulus of 115 MPa and 920-fold modulus increase. This phase separation-mediated dissipative approach significantly enhances the mechanical properties of transient materials with tunable lifetimes.

Introduction

Living systems are defined by their ability to generate ubiquitous, transient materials that operate far from thermodynamic equilibrium, constantly fueled by an influx of energy.[1] This complex, non-equilibrium dynamic behavior enables biological materials to autonomously adapt to environmental changes, a mechanism crucial for the sustainability of life.[2] Muscle provides a classic example: it contracts and stiffens in response to adenosine triphosphate (ATP)-fueled sliding of actin and myosin filaments, then spontaneously recovers to its resting soft state.[3] Inspired by this natural phenomenon, a variety of artificial transient materials fueled by chemicals, light, or force have been recently developed, with their mechanical, electrical, and optical properties being precisely controlled over time.[4–12] Such dissipative networks make these materials compelling for diverse applications with tunable lifetimes, including dissipative self-assembly,[6,13–15] molecular machines,[16] actuation,[17] adhesion,[18] transportation,[19] nanoreactors,[20] polymerization,[21] and patterning.[22,23]

In contrast to traditional modulus-adaptive materials that switch their stiffness at equilibrium states, chemical-fueled transiently stiffened materials have garnered particular interest due to its mimicry of muscle stiffening.[24] This behavior is generally achieved by employing two antagonistic reactions—an activation reaction and a deactivation reaction with different reaction rates—to drive the dissipative formation of crosslinking bonds, leading to the transient gelation or toughening of polymer networks.[13,17,18,23,25,26] For instance, carbodiimides can act as chemical fuels, creating hydrolytically unstable anhydrides from carboxylic acids in water. These anhydrides crosslink polymer chains to enhance stiffness, before autonomously hydrolyzing back to the original carboxylic acids, thus restoring the material's initial state.[23,26–29]

However, despite significant progress in this field, a major limitation persists: even in their stiffened state, current transient materials remain very soft (modulus <1 MPa). This strongly contrasts with the highly stiffened contractive muscles, thereby severely restricting their practical use in load-bearing applications. We ascribed this issue to the relatively homogeneous structure or simply supramolecular assemblies of existing transient materials, which only allow for gentle stiffening within viscous sol and rubbery gel regimes. It appears that simply altering crosslinking density is insufficient to induce the dramatic stiffening required. While introducing recrystallization or deswelling events can induce time-dependent dramatic stiffening, these processes compromise the materials' ability to operate repeatedly and autonomously.[30,31] This dilemma highlights the need for a new working mechanism capable of driving transient materials to stiffen into a rigid glassy state.

To address this problem, in this work, we propose to couple non-equilibrium chemistry with vitrifiable phase separation to achieve chemical fuel-driven dramatic stiffening

[*] Y. Zhao, Prof. S. Sun, Prof. P. Wu
State Key Laboratory of Advanced Fiber Materials, College of Chemistry and Chemical Engineering & Center for Advanced Low-dimension Materials, Donghua University, Shanghai 201620, China
E-mail: shengtongsun@dhu.edu.cn
wupeiyi@dhu.edu.cn
Dr. B. Wu
Jülich Centre for Neutron Science (JCNS) at Heinz Maier-Leibnitz Zentrum (MLZ) Forschungszentrum Jülich, Lichtenbergstr. 1, Garching 85748, Germany

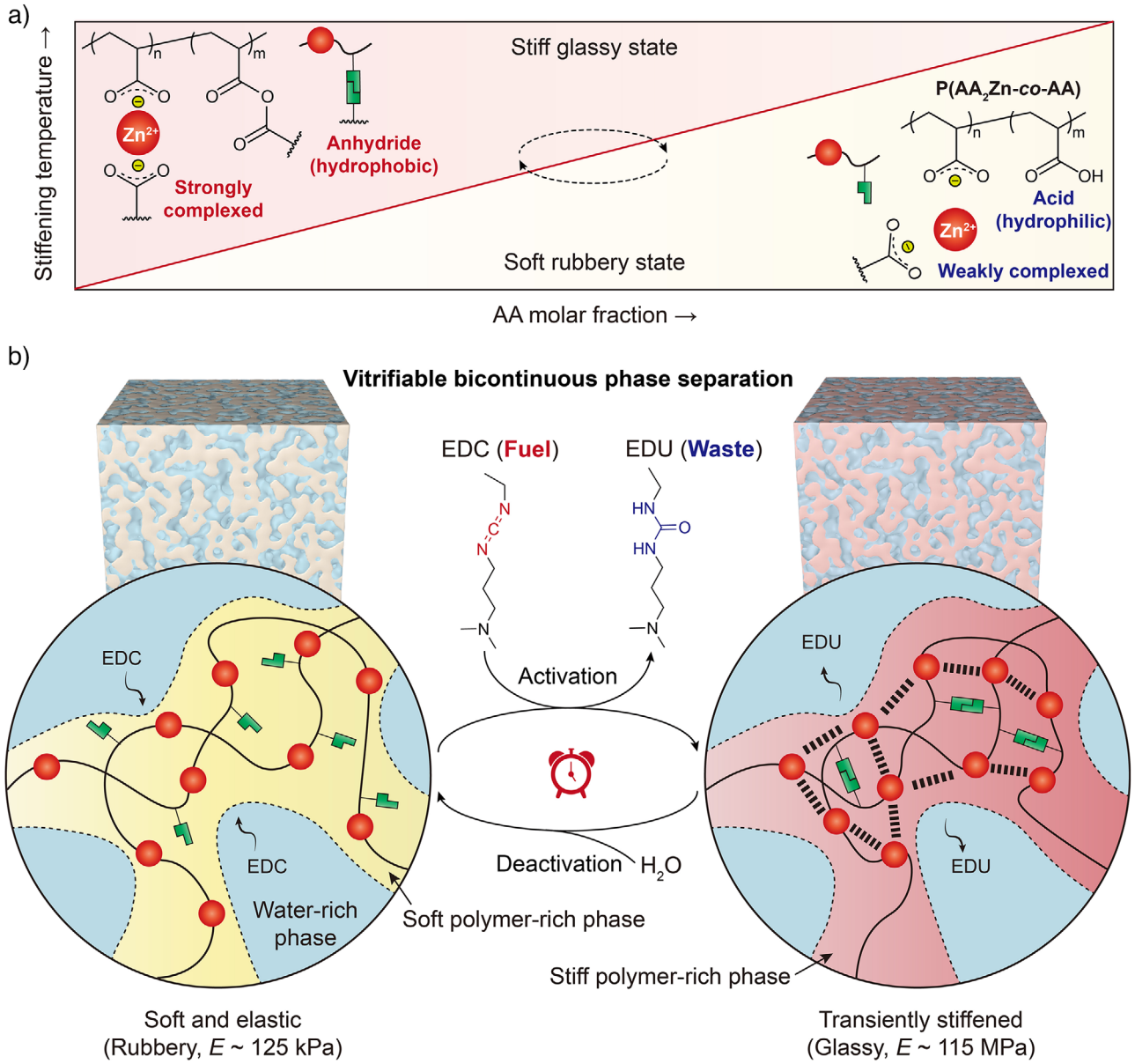

Figure 1. Working mechanism of chemical fuel-driven dramatic stiffening of transient hydrogels. a) Schematic phase diagram of P(AA_2Zn-*co*-AA) hydrogels. The stiffening temperature increases with a higher molar fraction of AA units. Consequently, the EDC-fueled conversion of hydrophilic AA units into hydrophobic anhydrides can significantly reduce the stiffening temperature, causing a dramatic transition from a soft rubbery state to a stiff glassy state under ambient conditions. b) Schematic transient stiffening process of P(AA_2Zn-*co*-AA) hydrogel. Bicontinuous phase separation occurs within the copolymer hydrogel. EDC as a chemical fuel diffuses freely in the water-rich phase and induces the transient vitrification of polymer-rich phase by converting AA units into anhydrides. Subsequently, the autonomous hydrolysis of anhydrides drives the system back to its original soft state with a tunable lifetime. Notably, the hydrogel's volume remains constant throughout the entire process, with only its stiffness changing.

of transient materials. Experimentally, we synthesized a thermal-stiffening copolymer hydrogel, which consists of thermal-stiffening zinc acrylate (AA_2Zn) units and transiently reactive acrylic acid (AA) units (Figure 1a). The stiffening temperature is defined by the crossover point between the lower critical solution temperature (LCST)-type spinodal curve and glass transition curve. Above this temperature, the hydrogel's phase separation is transiently arrested, inducing a dramatic transition from a rubbery/viscous state to a glassy state.[32] Crucially, the stiffening temperature of the copolymer hydrogel can be precisely tuned with a linear increase with the molar fraction of hydrophilic AA units. Under ambient conditions, the hydrogel undergoes a bicontinuous phase separation, partitioning into a soft polymer-rich phase and an interconnected water-rich phase (Figure 1b). However, with a controlled dose of 1-ethyl-3-(3-dimethylaminopropyl) carbodiimide (EDC), a chemical fuel, the AA groups are converted into hydrophobic anhydrides. This conversion significantly lowers the stiffening temperature to below room temperature, which in turn induces the instant and isochoric, yet transient, vitrification of polymer-rich phase. As a result, the optimized hydrogel transitions from a soft elastic state

($E \sim 125$ kPa) to a transiently stiffened glassy state ($E \sim 115$ MPa), with a remarkable 920-fold increase in Young's modulus. Over time, the glassy polymer-rich phase dissipates, returning to its original soft elastic state. The lifetime of this dissipative behavior can be finely modulated by the EDC concentration, and the transient process is repeatable for at least 9 cycles.

While carbodiimide-driven non-equilibrium chemistry is well-established, prior transient hydrogels have relied on either supramolecular assemblies or stimuli-inert polymer networks.[10,23,26,27,33] Consequently, their modulus changes were confined to soft viscous and rubbery regimes, with maximum moduli below 1 MPa. Similarly, introducing other fuels, such as chemicals, light, electricity, or mechanical forces, to comparable dissipative systems also failed to produce a truly rigid material.[5,13,34,35] This work, therefore, highlights the critical role of vitrifiable phase separation in transient hydrogels. This mechanism significantly amplifies modulus changes by leveraging highly sensitive phase structures. We present the first example of a transient material that can be reversibly stiffened into a glassy state through a fuel-driven process. This breakthrough marks a significant advance for life-like load-bearing and shape-memory applications.

Results and Discussion

Thermal-Stiffening and Fuel-Induced Stiffening Properties

Thermal-stiffening hydrogels were deliberately chosen as the model system for transiently stiffened materials due to their highly sensitive phase behavior and high mechanical strength in the stiffened state.[36] In contrast to conventional materials that typically soften with increasing temperature, thermal-stiffening hydrogels undergo spontaneous LCST-type phase separation and vitrification. This concurrent process leads to their instantaneous stiffening, a property that has found important applications in impact protection,[32] shape memory,[37] and adaptive lubrication.[38,39] Ca^{2+}-coordinated PAA hydrogels are a prime example of thermal-stiffening hydrogels, owing to the reduced aqueous solubility of Ca^{2+}:COO^- complexes at elevated temperatures.[32,40,41] However, our work requires a thermal-stiffening hydrogel with a tunable stiffening temperature below and above room temperature to enable chemical fuel-driven transient stiffening under ambient conditions. Unfortunately, although the stiffening temperatures of conventional Ca^{2+}-coordinated PAA hydrogels can be tuned by modulating their chemical structures,[40,42] they consistently remain above 40 °C, which does not meet our requirements.

In this work, we developed Zn^{2+}-coordinated PAA hydrogels that function as a thermal- and fuel-induced stiffening material with a significantly reduced stiffening temperature. Experimentally, we synthesized P(AA_2Zn-*co*-AA) copolymer hydrogels via the direct UV-initiated copolymerization of AA_2Zn and AA monomers in water at room temperature (see experimental details in the Supporting Information). Subsequent swelling in water produced hydrogels with varied AA molar fractions (relative to the total acrylate content) ranging from 0% to 30%. The hydrophilic AA units were included to both fine-tune the stiffening temperature and serve as the reactive groups for EDC-fueled transient reactions. Despite the absence of a conventional chemical crosslinker, possible chain transfer during polymerization resulted in a chemically crosslinked copolymer network that only swelled in 1 M HCl solution (Figure S1). All copolymer hydrogels appeared opaque at room temperature (25 °C), suggesting the occurrence of spontaneous phase separation (Figure 2a). Furthermore, the hydrogel became progressively softer with an increasing AA molar fraction, which indicates a corresponding increase in the stiffening temperature.

We evaluated the thermal-stiffening behavior of all copolymer hydrogels using temperature-sweep rheology (Figure S2). The neat PAA_2Zn hydrogel exhibited an apparent thermal-stiffening behavior with a stiffening temperature of approximately 5 °C, which was determined by the peak of the loss factor, tan δ (where tan δ is the ratio of the loss moduli, G″, to storage moduli, G″), as shown in Figure 2b. Increasing AA molar fraction shifted the stiffening temperature to higher values; for an AA molar fraction of 6% (i.e., P(AA_2Zn-co-AA6%), the stiffening temperature equals to 30.5 °C. This dramatic transition switched the hydrogel from a soft, rubbery state at lower temperatures to a stiff, glassy state at higher temperatures, a phenomenon also confirmed by distinct tensile stress-strain curves at 25 and 80 °C, respectively (Figure S3). The maximum thermal-stiffening response was observed at an AA molar fraction of 6%, with 138-fold increase in storage modulus (G″) and 428-fold increase in Young's modulus (E) from 25 to 80 °C (Figure S4). We plotted the phase diagram of the copolymer hydrogel, which illustrates the stiffening temperatures as a function of AA molar fraction (Figure 2c). A linear relationship was observed with a slope of 4.7 °C $\%^{-1}$, indicating the fine tunability of the stiffening temperature. Consequently, by converting AA units into hydrophobic anhydrides, a dramatic phase transition from a rubbery to a glassy state can be expected at the constant room temperature.

Building on this hypothesis, we examined the EDC fuel-induced stiffening behavior of the copolymer hydrogels. To eliminate the effects of concentration gradient and transient reaction on the measured mechanical properties, we soaked the hydrogels in a sufficient amount of 1 M EDC solution for 30 min. This ensured the complete conversion of AA units to anhydrides, a process that simulates localized stiffening in practical applications. The full conversion of AA units to anhydrides was confirmed by IR spectral analysis (Figure S5). We did not use buffer solutions to control pH, as common buffer salts like phosphates and 4-morpholineethanesulfonic acid (MES) may strongly coordinate with the Zn^{2+} in the hydrogel. Fortunately, the EDC solutions was found to be near neutral, which would not significantly alter the hydrogel's pH. Benefiting from the microsyneresis mechanism of thermal-stiffening hydrogels,[32,40,41] the volume of P(AA_2Zn-*co*-AA) hydrogels remained almost unchanged after EDC soaking (Figures 2d, S6, S7). Importantly, all the investigated hydrogels exhibited significant stiffening after soaking in the EDC solution. Although the stiffening process initiated from the surface, the interconnected water channels within the

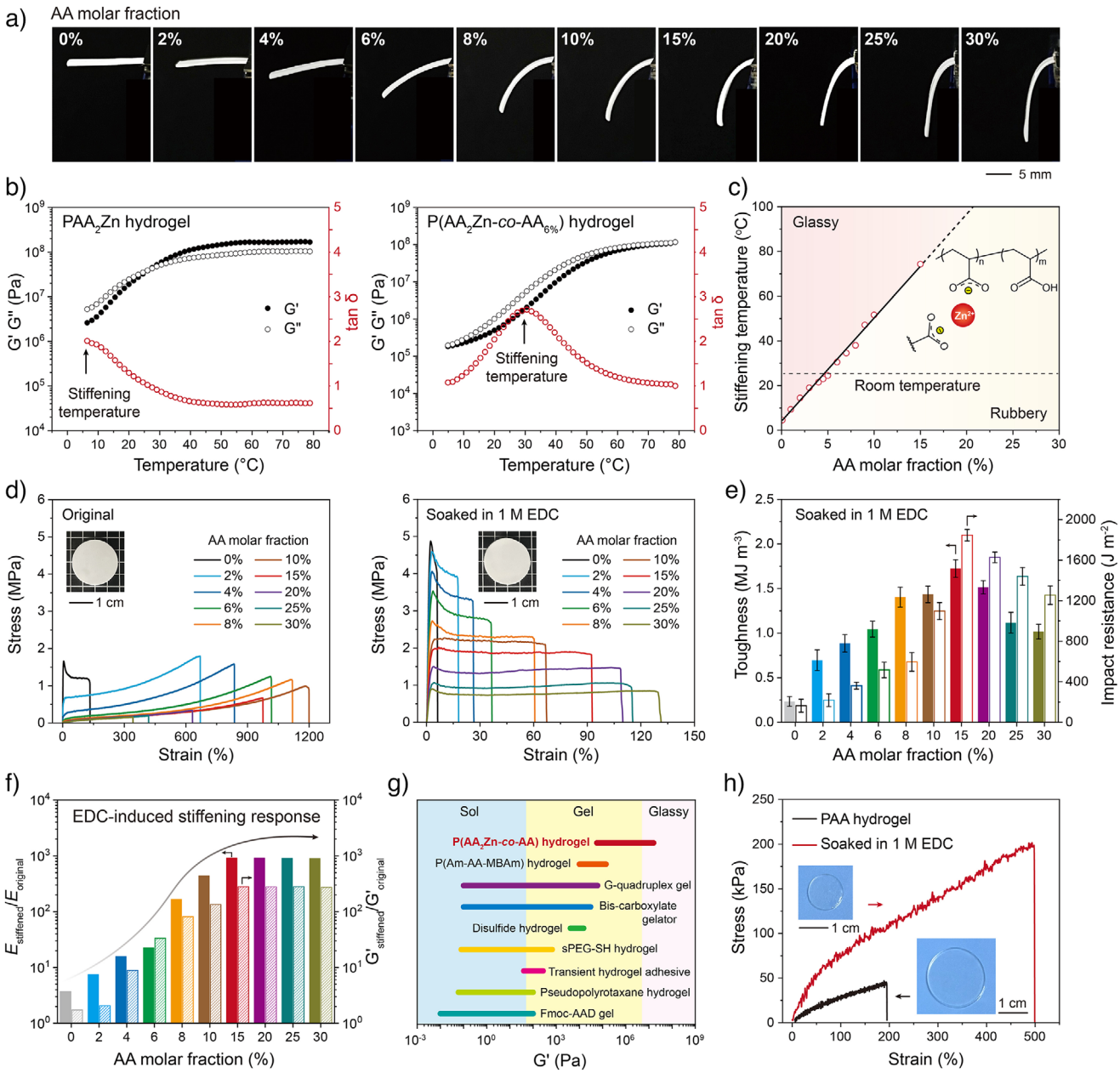

Figure 2. Thermal-stiffening and fuel-induced stiffening properties. a) Photos of P(AA_2Zn-*co*-AA) hydrogels with increasing AA molar fractions. b) Temperature-sweep rheological curves of PAA_2Zn and P(AA_2Zn-*co*-$AA_{6\%}$) hydrogels (collected at 0.1 Hz). c) Phase diagram of P(AA_2Zn-*co*-AA) hydrogels by plotting the relationship between stiffening temperature and AA molar fraction. d) Tensile stress-strain curves of P(AA_2Zn-*co*-AA) hydrogels before and after soaking in 1 M EDC (insets: corresponding photos in the two states). e) Toughness and impact resistance as a function of AA molar fraction. f) EDC fuel-induced stiffening response, as evaluated by the change ratio of Young's modulus and storage modulus between the stiffened and original states. g) Comparison of the stiffening response among typical transiently stiffened materials. h) Tensile stress-strain curves of PAA hydrogels before and after soaking in 1 M EDC (insets: corresponding photos in the two states).

stiffened "hydrogel skin" facilitated the continuous diffusion of EDC fuels, resulting in a homogeneous stiffened material with highly reproducible stress-strain curves (Figure S8). We calculated the toughness and impact resistance of the stiffened copolymer hydrogels with varying AA molar fractions. Despite a reduction in Young's modulus with an increasing AA molar fraction in the stiffened state, the hydrogel with 15 mol% AA showed a maximum toughness (~1.72 MJ m^{-3}) and impact resistance (~1846 J m^{-2}) (Figure 2e). The consistently high toughness and impact resistance imply the great potential of P(AA_2Zn-*co*-AA) hydrogels in load-bearing and impact-protecting applications.[40,43,44]

We further evaluated the EDC fuel-induced stiffening response, quantifying the changes in both Young's and storage moduli (Figure 2f; see time-sweep rheological data in Figure S9 and corresponding moduli in Figure S10). The stiffening response increased with a higher AA molar fraction, reaching a plateau when the AA molar fraction

exceeded 15%. This can be understood as an effect where more AA units facilitate a more significant structural change and a more dramatic phase transition in the hydrogel network. However, higher AA molar fractions also led to a reduced proportion of the thermal-stiffening AA_2Zn units, which ultimately prevented a further enhanced fuel-induced stiffening response. Therefore, unless otherwise stated, all copolymer hydrogels discussed hereafter refer to the hydrogel with an AA molar fraction of 15%. At this composition, the stiffening response reached a remarkable 920-fold increase in Young's modulus, transitioning from an ultrasoft state (E ~125 kPa) to a highly stiffened state (E ~ 115 MPa). Rheological data yielded similar results, showing a 280-fold increase in storage modulus.

To highlight the advantage of our design, we compared the fuel-driven stiffening response of P(AA_2Zn-*co*-$AA_{15\%}$) hydrogel with previous transiently stiffened materials, as shown in Figure 2g (see corresponding data in Table S1; rheological data were adopted for accurate comparison). Despite their diverse fuel types and chemical systems, earlier transient materials consistently showed modulus changes within the soft viscous and rubbery gel regimes. While the modulus change ratio of these materials may be vast (e.g., up to 6 × 10^5 times for G-quadruplex hydrogel),[35] their maximum moduli were consistently below 1 MPa, which are insufficient for practical load-bearing applications. This limitation stems from their synthesis, which is typically based on either supramolecular assemblies of small molecules or relatively homogeneous polymer networks, neither of which can effectively freeze chain movements through fuel-induced intermolecular crosslinking. In stark contrast, our approach leverages vitrifiable phase separation to enable a transient copolymer hydrogel to switch between a soft rubbery state and a rigid glassy state. This innovation results in an increase in storage modulus from 5.64×10^4 Pa to a record-high value of 1.58×10^7 Pa. This unprecedented stiffened modulus marks the first time a fuel-driven transient material has achieved a truly rigid, glassy state. As a control, we also prepared a homogeneous chemically crosslinked PAA hydrogel and soaked it in 1 M EDC solution to achieve the full conversion of AA units into anhydrides. Unlike P(AA_2Zn-*co*-AA) hydrogel, this neat PAA hydrogel suffered a significant 83% volume contraction and remained soft, with a low Young's modulus of only 79 kPa (Figure 2h). These results collectively highlight the importance of vitrifiable phase separation in achieving chemical fuel-driven stiffening with both a dramatic response and a constant volume.

Fuel-Driven Transient Stiffening Behavior

We first investigated the influence of EDC dose on the stiffening behavior of P(AA_2Zn-*co*-AA) hydrogel. As a lower EDC dose can only convert partial AA units into anhydrides, it should lead to a correspondingly lower stiffening response. Indeed, the viscoelasticity of the stiffened copolymer hydrogel can be finely tuned by varying EDC concentration, as evidenced by the time-concentration superposition rheology (Figure 3a). To ensure complete reaction, all hydrogel samples for rheological tests were pre-immersed in sufficient EDC solution for 30 min at various concentrations. The original copolymer hydrogel, without EDC treatment, located in a typical rubbery regime. However, increasing EDC concentration from 0.05 to 4 M gradually transformed the stiffened hydrogel into dissipating (i.e., glass transition) and glassy states, accompanied by a significant increase in storage moduli by more than three orders of magnitude. A critical concentration of 0.25 M was observed, above which the stiffened hydrogel fully entered the glassy state. Tensile measurements yielded very similar results, showing an increase in Young's moduli with increasing EDC concentrations (Figure 3b,c). When the EDC concentration exceeded 0.25 M, the tensile curve exhibited an apparent yielding behavior, indicative of the formation of a glassy phase.

The preceding results revealed that adjusting EDC dose can control the fuel-induced stiffening response of the copolymer hydrogel. Consequently, we hypothesized that if an insufficient amount of EDC was introduced to the hydrogel, the antagonistic activation and deactivation reactions would compete to induce transient stiffening. To confirm this, we dosed a hydrogel sample (~0.17 g) with 0.05 mmol of EDC (50 µL of 1 M EDC) and measured the resulting transient changes in mechanical properties (Figure 3d). Upon EDC dosing, the original soft and elastic hydrogel transitioned to a stiff state with a Young's modulus of 13 MPa. Note that, this value is considerably lower than the maximum Young's modulus of 115 MPa, which was achieved when all AA units were converted to anhydrides. Although the bulk hydrogel remained soft, the stiffening of the hydrogel's outer layer was sufficient to induce a significant modulus increase of the entire material. After resting for 1 h, the stiffened hydrogel recovered to a soft state. The incomplete recovery is attributed to the presence of 1-ethyl-3-(3-dimethylaminopropyl)urea (EDU) byproduct, a persistent issue in current closed artificial transient systems.[23,24,27,45] This contrasts with living open systems, which can continuously remove metabolic waste via fluid circulation, thereby fully refreshing the non-equilibrium cycle.[1]

We then studied the cyclability of the transient stiffening behavior of the copolymer hydrogel. For this purpose, we delivered 0.1 mmol EDC (100 µL of 1 M EDC) below a copolymer hydrogel disk (diameter ~2 cm, thickness ~1 mm) and immediately monitored the modulus changes via a rheometer. As demonstrated in Figure 3e, upon EDC addition, both the storage and loss moduli significantly increased within 20 min, indicating a fuel-induced stiffening response. However, over the period of 1 h, the moduli reduced to lower values, corresponding to the autonomous recovery of the hydrogel. Repeating this process induced very similar changes, and the transient stiffening response could be cycled for at least 9 times. A notable observation was the slight increase in the recovered hydrogel's modulus with each successive cycle. The absence of anhydride-related peaks in the infrared (IR) spectrum after modulus recovery rules out incomplete anhydride hydrolysis as the cause (Figure S11). Instead, we attribute this phenomenon to also the accumulation of EDU byproduct. This is supported by the increased recovered modulus when EDU was pre-supplied to the EDC

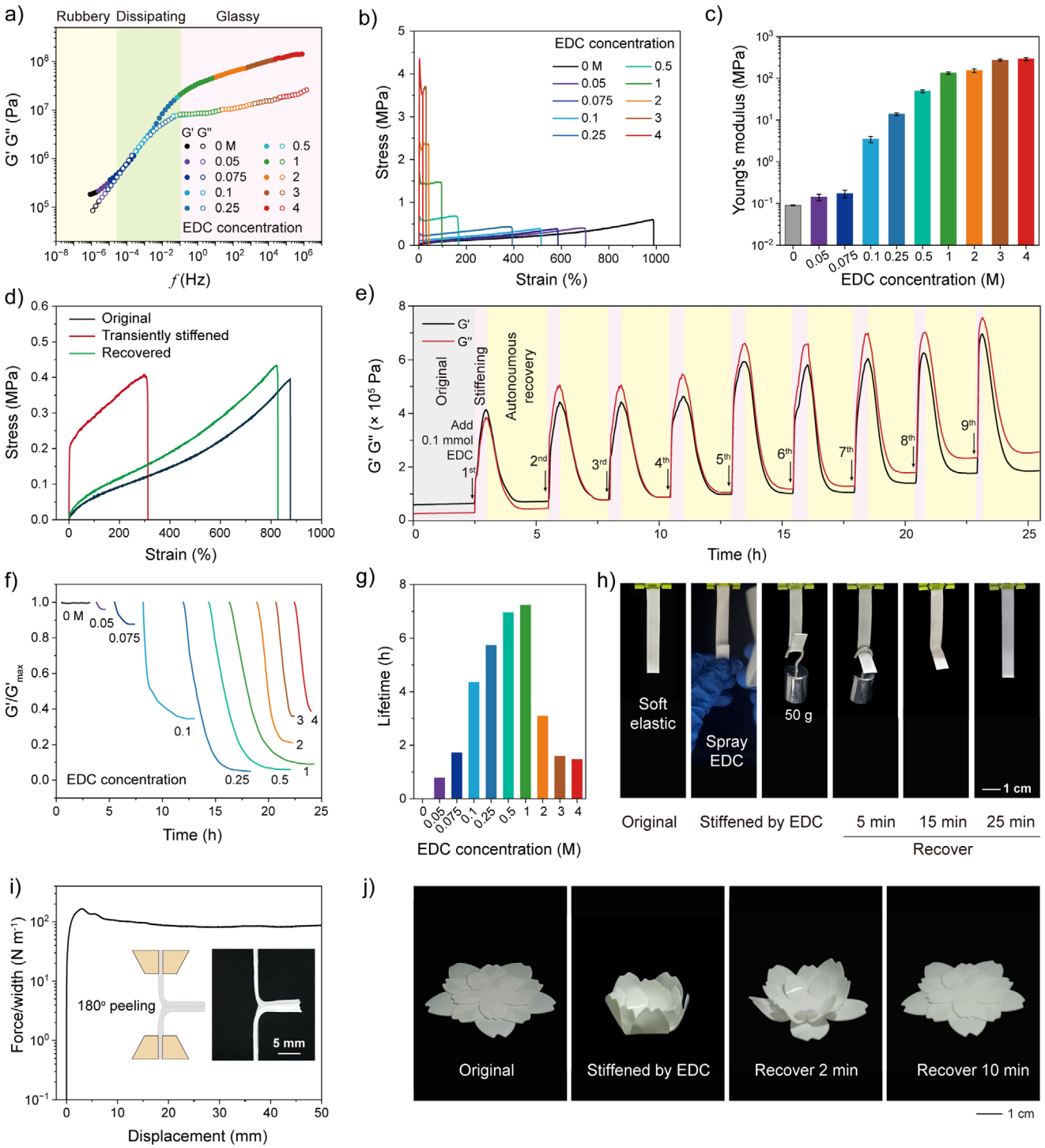

Figure 3. Chemical fuel-driven transient stiffening properties. a) Time-concentration superposition rheology curves of P(AA_2Zn-*co*-$AA_{15\%}$) hydrogel treated with various concentrations of EDC (reference concentration: 1 M). b) Tensile stress-strain curves of the hydrogels treated with various concentrations of EDC. c) Corresponding Young's moduli. d) Tensile stress-strain curves of the hydrogels in the original, transiently stiffened (add 0.05 mmol EDC), and recovered states. e) Cycled transient stiffening properties monitored by rheology by repeatedly adding EDC fuel. f) Time-dependent normalized storage modulus recovery curves. g) Calculated lifetimes as a function of EDC concentration. h) EDC-fueled temporary load-bearing of a hydrogel strip. i) 180° peeling curve of two adhered hydrogels using acetic acid. j) EDC-fueled temporary shape memory of an adhered hydrogel flower.

fuel solution (Figure S12). As EDU is more basic than EDC, it likely strengthens the Zn^{2+}:COO^- complexation, leading to a higher physical crosslinking strength.

We further demonstrated that the lifetime of the transient stiffening response can be modulated by EDC concentration. We monitored the recovery of normalized storage moduli of the stiffened copolymer hydrogel at different EDC concentrations (Figure 3f). While a low EDC concentration resulted in minor modulus changes, excessively high concentrations also compromised the transient modulus recovery properties. Here, the transient stiffening lifetime was defined as the time required for the modulus to recover to 90% of its maximum value.[23] The calculated lifetime first increased from 0.8 h for 0.05 M EDC to 7.2 h for 1 M EDC, before gradually decreasing to 1.2 h for 4 M EDC (Figure 3g). This nonlinear behavior is likely because excess EDC generated more basic EDU waste, which raised the hydrogel's pH and accelerated anhydride hydrolysis.

To demonstrate the transient stiffening properties of the copolymer hydrogel, we sprayed a curved hydrogel strip with 4 M EDC solution and used it to support a 50 g weight (Figure 3h and Movie S1). As expected, the stiffened hydrogel strip gradually softened over time, releasing the weight and recovering its original soft state within 25 min. Owing to the physical crosslinking nature of AA_2Zn units, two hydrogel films could be tightly adhered with acetic acid. Subsequent removal of acetic acid by immersion in water resulted in a high interfacial toughness of ca. 167 J m^{-2}, as evaluated by 180° peeling test (Figure 3i). Using this method, we prepared a hydrogel flower by adhering three hydrogel petals, and the flower could then be stiffened into a closed state by spreading 2 M EDC solution (Figure 3j). Over time, the hydrogel flower autonomously recovered to its original open state within 10 min (Movie S2). These results collectively suggest the hydrogel's transient stiffening and recovering properties, which cannot be easily achieved by previous transient materials with a moderate stiffening response. Moreover, given its simple preparation, our transient copolymer hydrogel can be produced in various shapes and on a large scale. The EDC fuel can also be applied in diverse ways, including soaking, spraying, atomizing, and site-specific spreading. All these features make the copolymer hydrogel highly applicable in a variety of smart scenarios, such as transient impact protection,[32,43] modulus-adaptive sensing,[46] and soft robotics.[47]

Mechanism Discussion for Water-Activated Self-Adhesion

To gain deeper insights into the EDC fuel-driven transient stiffening behavior, we investigated the temporary phase separation process using scanning electron microscopy (SEM) and atomic force microscopy (AFM). The samples for SEM were prepared by quenching the evolving phase structure with liquid nitrogen, followed by freeze-drying. The original copolymer hydrogel exhibited a typical bicontinuous morphology with a clear boundary between the polymer-rich phase (acts as a structural framework) and water-rich phase (forms interconnected nanopores) (Figure 4a). The water-rich phase can serve as a fast-transport channel for the diffusion of EDC fuel and EDU waste, which in turn facilitates the rapid stiffening and time-dependent recovery of the hydrogel. EDC treatment did not disrupt the bicontinuous structure, yet coarsened and solidified the polymer-rich phase, indicating the occurrence of transient stiffening. After 2 h recovery, the polymer phase reverted to a smoother morphology. The phase boundary, however, appeared slightly blurred, likely due to the accumulation of EDU waste. Similar transient stiffening-induced structural changes were clearly evidenced by AFM observations (Figure 4b). The AFM phase image, which is based on phase shifts in tapping mode, can be used to distinguish the lateral distribution of mechanical properties on the material surface. Consistent with SEM observations, all the three states of the hydrogel sample exhibited typical bicontinuous phase structures. Nevertheless, in contrast to the original and recovered samples, the transiently stiffened sample possessed a much more solidified polymer-rich phase, again confirming that the dramatic stiffening response originates from the vitrification of polymer-rich phase.

To elucidate the internal structure of the vitrified polymer-rich phase, we conducted small-angle X-ray scattering (SAXS) measurements. The curve-fitted SAXS profiles for both the transiently stiffened and original samples displayed similar features in the low-q region, following Porod scattering of $I \propto q^{-4}$ (Figure 4c). This indicates that the macroscopic structure of the two samples remained largely unchanged. However, a pronounced upturn was observed in the high-q region of the transiently stiffened sample, which we attribute to the formation of rigid clusters with a radius of gyration (R_g) of approximately 3 nm. Furthermore, the appearance of these rigid clusters increased the average mesh size of the hydrogel from 0.5 to 1.5 nm, suggesting chain reorganization and cluster coalescence within the polymer-rich phase. This clustered architecture was further confirmed by transmission electron microscopy (TEM) and AFM images, which revealed similar cluster sizes (Figures 4c and S13). All these findings suggest that the vitrified polymer-rich phase is actually formed by the close packing of stiffening PAA_2Zn clusters. The emergence of these stiffening clusters has also been observed in previous thermal-stiffening PAA_2Ca hydrogels, indicating a similar stiffening mechanism.[40] Mechanistically, the EDC-induced conversion of AA units into anhydrides promotes the formation of numerous dehydrated PAA_2Zn clusters, which subsequently coalesce into larger glassy phases. As the anhydrides hydrolyze back to AA units over time, the clusters rehydrate and the glassy phases dissolve. This dynamic, reversible, and dissipative assembly of PAA_2 Zn clusters at the nanoscale is responsible for the macroscopic, transient changes in modulus.

To further elucidate the internal dynamics, we employed 2D low-field ^1H nuclear magnetic resonance (NMR) spectroscopy to investigate how water mobility changes upon EDC treatment (Figure 4d). In the 2D T_1-T_2 map (T_1: spin-lattice relaxation time; T_2: spin-spin relaxation time), the T_1/T_2 ratio reflects the molecular mobility of H-containing species.[48,49] Generally, a low T_1/T_2 ratio indicates higher mobility, with the diagonal line $T_1/T_2 = 1$ corresponding to a fully mobile state. In both the original and transiently

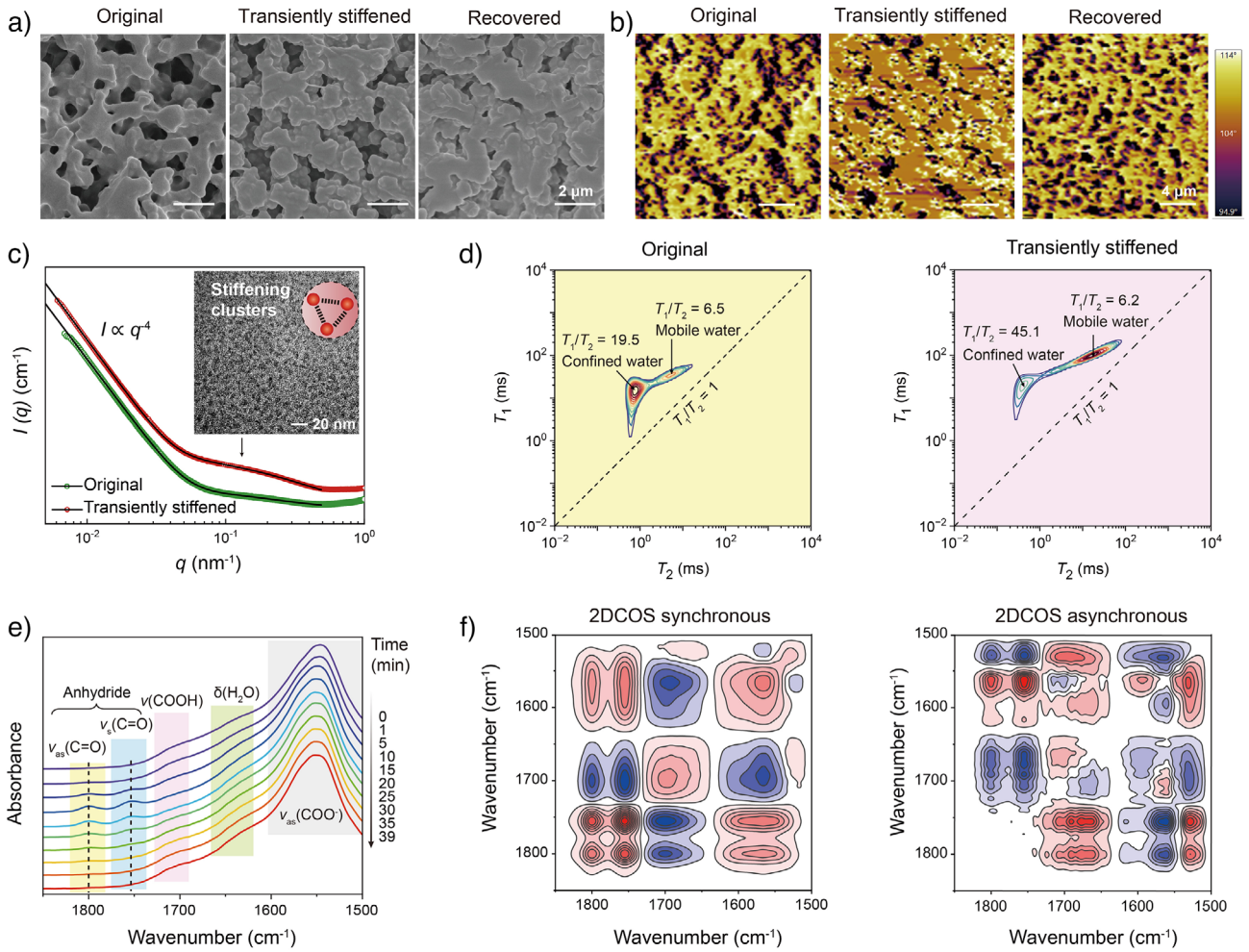

Figure 4. Mechanism discussion for EDC fuel-driven transient stiffening. a) SEM morphology and b) AFM phase images of P(AA_2Zn-*co*-$AA_{15\%}$) hydrogel in its original, transiently stiffened, and recovered states. c) Curve-fitted SAXS profiles of the copolymer hydrogel in its original and transiently stiffened states, based on the correlation length model. The inset shows a TEM image of the stiffened hydrogel, confirming the presence of numerous stiffening clusters. d) 2D low-field ^{1}H NMR spectra of the copolymer hydrogel in the original and transiently stiffened states. e) Stacked time-resolved ATR-FTIR spectra of the hydrogel during EDC diffusion. f) 2DCOS synchronous and asynchronous spectra generated from the time-resolved spectra. In 2DCOS spectra, red colors represent positive intensities, while blue colors represent negative intensities.

stiffened states, 2D low-field NMR distinguished two classes of water: confined water in the polymer-rich phase with a higher T_1/T_2 ratio, and mobile water in the water-rich phase with a lower T_1/T_2 ratio. The interconnection of these two peaks suggests their exchangeable dynamics.[50] Notably, EDC treatment significantly reduced the molecular mobility of the confined water, while the mobile water remained largely unaffected. This finding confirms that the EDC-induced transient stiffening primarily occurs within the polymer-rich phase by generating a more confined network.

Finally, we conducted attenuated total reflectance Fourier-transform infrared (ATR-FTIR) spectroscopy measurements to monitor the subtle molecular changes that occurred during the transient stiffening process. Time-resolved FTIR spectra were collected at the ATR crystal-hydrogel interface as EDC diffused through the hydrogel film (see experimental setup in Figure S14). This approach allowed us to trace the transient changes of all relevant chemical groups. Specifically, we monitored the asymmetric and symmetric C═O stretching of anhydride (at 1800 and 1755 cm^{-1}, respectively), the C═O stretching of carboxylic acid (COOH, ~1700 cm^{-1}), the O-H bending of water (~1650 cm^{-1}), and the asymmetric C═O stretching of carboxylate (COO^-, ~1550 cm^{-1}) (Figure 4e). Over time, the gradual emergence and disappearance of the anhydride-related peaks were clearly observed. This was accompanied by an initial reduction and subsequent increase in the COOH-related peaks, confirming the occurrence of transient reactions that involve the conversion of AA units into anhydrides followed by the hydrolysis of the anhydrides back to AA units. The inverse spectral intensity changes in the stiffening and recovery processes can be more clearly discerned in the overlapped IR spectra (Figure S15). Furthermore, difference spectra showed that the maximum spectral change occurred at 11 min, which corresponds to the most stiffened state of the material (Figure S16).

The entire spectra from the transient stiffening process were further analyzed using 2D correlation spectroscopy (2DCOS) to extract more subtle information about the

changing sequence (Figure 4f). Based on Noda's judging rule and the signs of cross-peaks in the synchronous and asynchronous spectra,[48,51] we established the following sequential order of events driven by EDC diffusion (→ means prior to or earlier than; see determination details in Table S2): 1755 cm^{-1} → 1800 cm^{-1} → 1594 cm^{-1} → 1701 cm^{-1} → 1563 cm^{-1} → 1661 cm^{-1} → 1531 cm^{-1}. This corresponds to the sequence of molecular vibrations: ν_s(C=O) (anhydride) → ν_{as}(C=O) (anhydride) → $\nu_{as}(COO^-)$ (free) → ν(COOH) → $\nu_{as}(COO^-)$ (weakly coordinated with Zn^{2+}) → δ(O-H) (confined H_2O) → $\nu_{as}(COO^-)$ (strongly coordinated with Zn^{2+}). The earliest response from anhydride-related vibrations indicates that the transient stiffening process is indeed driven by the EDC-induced conversion from COOH to anhydride. The subsequent responses from COO^- and confined water reveal the consequent vitrification of the polymer-rich phase.

Taken together, the transient stiffening of P(AA_2Zn-*co*-AA) hydrogel can be understood at two distinct length scales. At the mesoscale, EDC diffuses through the water-rich phase and induces the dramatic vitrification of the polymer-rich phase, which leads to the emergence of closely packed stiffening clusters. At the molecular level, these temporary changes are driven by the conversion of AA units into anhydrides, a mechanism that strongly supports our proposed hypothesis in Figure 1.

Conclusion

In this paper, we introduce a novel strategy that couples vitrifiable phase separation with non-equilibrium chemistry to significantly enhance the mechanical properties of transiently stiffened materials. Unlike traditional transient materials, which are based on either supramolecular assemblies or relatively homogeneous structures, our synthesized P(AA_2Zn-*co*-AA) copolymer hydrogel features a thermal-stiffening bicontinuous phase separation. The addition of EDC triggers the transient conversion of AA units into hydrophobic anhydrides, which dramatically reduces the stiffening temperature. This leads to the instant vitrification of polymer-rich phase, transforming the initial soft hydrogel into a stiff glassy state with an ultrahigh modulus of 115 MPa. We emphasize that this stiffened modulus is unparalleled among current artificial transient materials. Furthermore, the lifetime of this transient hydrogel can be finely tuned by adjusting EDC concentration. We anticipate that, this phase separation-mediated non-equilibrium chemistry will pave the way for creating advanced transient materials that more precisely mimic living systems.

Acknowledgements

This work was supported by the National Natural Science Foundation of China (52322306, 22275032, and 52433003) and the Shanghai Oriental Talent Program.

Conflict of Interests

The authors declare no conflict of interest.

Data Availability Statement

The data that support the findings of this study are available from the corresponding author upon reasonable request.

Keywords: Hydrogels · Non-equilibrium chemistry · Phase separation · Thermal-stiffening · Transient materials

[1] K. Das, L. Gabrielli, L. J. Prins, *Angew. Chem. Int. Ed.* **2021**, *60*, 20120–20143.
[2] R. Merindol, A. Walther, *Chem. Soc. Rev.* **2017**, *46*, 5588–5619.
[3] D. F. Cain, A. A. Infante, R. E. Davies, *Nature* **1962**, *196*, 214–217.
[4] Z. Wang, J. Xiao, T. Zhao, C. Zhang, L. Wang, N. He, Q. Kong, X. Wang, *Chem. Commun.* **2023**, *59*, 9818–9831.
[5] H. Ke, L.-P. Yang, M. Xie, Z. Chen, H. Yao, W. Jiang, *Nat. Chem.* **2019**, *11*, 470–477.
[6] S. Bianco, F. Hallam Stewart, S. Panja, A. Zyar, E. Bowley, M. Bek, R. Kádár, A. Terry, R. Appio, T. S. Plivelic, M. Maguire, H. Poptani, M. Marcello, R. R. Sonani, E. H. Egelman, D. J. Adams, *Nat. Synth.* **2024**, *3*, 1481–1489.
[7] X. Hao, K. Yang, H. Wang, F. Peng, H. Yang, *Angew. Chem. Int. Ed.* **2020**, *59*, 4314–4319.
[8] H. Xu, Q. Wang, Z. Qi, X. Li, Y. Lei, H. An, H. Tian, D.-H. Qu, *Angew. Chem. Int. Ed.* **2025**, *64*, e202420707.
[9] J. Li, F. Yin, J. Wang, H. Du, F. Xu, S. Meskers, Y. Li, S. Wijker, Y. Peng, R. Bellan, G. Vantomme, J. Song, C.-S. Liu, E. W. Meijer, *J. Am. Chem. Soc.* **2025**, *147*, 17361–17371.
[10] I. Tsironi, J. A. Maleszka, B. A. K. Kriebisch, R. S. Wilson-Kovacs, O. Acevedo, S. L. O'Leary, J. Watt, J. Boekhoven, J.-H. Olivier, *Angew. Chem. Int. Ed.* **2025**, *64*, e202417109.
[11] Y. Ren, A. Kravberg, S. Xie, E. S. Grape, Z. Yang, A. K. Inge, M. Yan, O. Ramström, *Aggregate* **2025**, *6*, e659.
[12] K. Chen, D. Ho, *Aggregate* **2024**, *5*, e425.
[13] J. Boekhoven, W. E. Hendriksen, G. J. M. Koper, R. Eelkema, J. H. van Esch, *Science* **2015**, *349*, 1075–1079.
[14] P. Zhao, Y. Zhao, Y. Lu, L. Xu, B. Li, Y. Zhao, W. Zhou, P. Yan, Y. Wang, K. Cao, Y. Zheng, *Angew. Chem. Int. Ed.* **2024**, *63*, e202409169.
[15] Q. Wang, Z. Qi, M. Chen, D.-H. Qu, *Aggregate* **2021**, *2*, e110.
[16] P. L. Wang, S. Borsley, M. J. Power, A. Cavasso, N. Giuseppone, D. A. Leigh, *Nature* **2025**, *637*, 594–600.
[17] R. Baretta, G. Davidson-Rozenfeld, V. Gutkin, M. Frasconi, I. Willner, *J. Am. Chem. Soc.* **2024**, *146*, 9957–9966.
[18] M. Li, G. Tian, X. Jiang, D. Qi, B. Yang, Y. Li, *Angew. Chem. Int. Ed.* **2025**, *64*, e202503010.
[19] H. Fu, N. Cao, W. Zeng, M. Liao, S. Yao, J. Zhou, W. Zhang, *J. Am. Chem. Soc.* **2024**, *146*, 3323–3330.
[20] S. Maiti, I. Fortunati, C. Ferrante, P. Scrimin, L. J. Prins, *Nat. Chem.* **2016**, *8*, 725–731.
[21] N. K. Saha, W. S. Salvia, D. Konkolewicz, C. S. Hartley, *Angew. Chem. Int. Ed.* **2024**, *63*, e202404933.
[22] H. Wang, X. Fu, G. Gu, S. Bai, R. Li, W. Zhong, X. Guo, R. Eelkema, J. H. van Esch, Z. Cao, Y. Wang, *Angew. Chem. Int. Ed.* **2023**, *62*, e202310162.
[23] C. W. H. Rajawasam, C. Tran, M. Weeks, K. S. McCoy, R. Ross-Shannon, O. J. Dodo, J. L. Sparks, C. S. Hartley, D. Konkolewicz, *J. Am. Chem. Soc.* **2023**, *145*, 5553–5560.
[24] C. W. H. Rajawasam, D. Konkolewicz, C. S. Hartley, *ChemSystemsChem* **2025**, *7*, e202400090.
[25] R. Baretta, M. F. Pantano, M. Frasconi, *Adv. Funct. Mater.* **2025**, *35*, 2502531.
[26] C. W. H. Rajawasam, C. Tran, J. L. Sparks, W. H. Krueger, C. S. Hartley, D. Konkolewicz, *Angew. Chem. Int. Ed.* **2024**, *63*, e202400843.

[27] L. S. Kariyawasam, C. S. Hartley, *J. Am. Chem. Soc.* **2017**, *139*, 11949–11955.
[28] M. Tena-Solsona, B. Rieß, R. K. Grötsch, F. C. Löhrer, C. Wanzke, B. Käsdorf, A. R. Bausch, P. Müller-Buschbaum, O. Lieleg, J. Boekhoven, *Nat. Commun.* **2017**, *8*, 15895.
[29] W. S. Salvia, G. Mantel, N. K. Saha, C. W. H. Rajawasam, D. Konkolewicz, C. S. Hartley, *Chem. Commun.* **2024**, *60*, 12876–12879.
[30] X. Zhang, Y. Zhou, H. Chen, Y. Zheng, J. Liu, Y. Bao, G. Shan, C. Yu, P. Pan, *Adv. Mater.* **2025**, *37*, e2500295.
[31] Y. Zhang, S. Ye, Y. Yang, R. He, J. Lin, Z. Hong, C. Yuan, L. Dai, *Adv. Funct. Mater.* **2025**, *35*, 2424535.
[32] T. Nonoyama, Y. W. Lee, K. Ota, K. Fujioka, W. Hong, J. P. Gong, *Adv. Mater.* **2020**, *32*, 1905878.
[33] Z. Zong, Q. Zhang, S.-H. Qiu, Q. Wang, C. Zhao, C.-X. Zhao, H. Tian, D.-H. Qu, *Angew. Chem. Int. Ed.* **2022**, *61*, e202116414.
[34] R. Baretta, M. Frasconi, *J. Am. Chem. Soc.* **2024**, *146*, 7408–7418.
[35] X.-Q. Xie, Y. Zhang, Y. Liang, M. Wang, Y. Cui, J. Li, C.-S. Liu, *Angew. Chem. Int. Ed.* **2022**, *61*, e202114471.
[36] Y. Yang, Y. Ru, T. Zhao, M. Liu, *Chem* **2023**, *9*, 3113–3137.
[37] C. Ni, D. Chen, Y. Yin, X. Wen, X. Chen, C. Yang, G. Chen, Z. Sun, J. Wen, Y. Jiao, C. Wang, N. Wang, X. Kong, S. Deng, Y. Shen, R. Xiao, X. Jin, J. Li, X. Kong, Q. Zhao, T. Xie, *Nature* **2023**, *622*, 748–753.
[38] Y. Zhang, W. Zhao, S. Ma, H. Liu, X. Wang, X. Zhao, B. Yu, M. Cai, F. Zhou, *Nat. Commun.* **2022**, *13*, 377.
[39] J. Chai, Y. Ru, Y. Jia, Y. Yang, H. Zhang, L. Chen, T. Zhao, M. Liu, *Adv. Mater.* **2025**, *37*, 2416250.
[40] L. Li, B. Wu, S. Sun, P. Wu, *Natl. Sci. Rev.* **2025**, *12*, nwaf072.
[41] J. Wu, B. Wu, J. Xiong, S. Sun, P. Wu, *Angew. Chem. Int. Ed.* **2022**, *61*, e202204960.
[42] Z. Yuan, Y. Jin, Y. Wu, X. Wu, N. Hai, J. Lu, C. Zhao, J. Zhang, *Macromolecules* **2024**, *57*, 7798–7807.
[43] H. Qiao, B. Wu, S. Sun, P. Wu, *J. Am. Chem. Soc.* **2024**, *146*, 7533–7542.
[44] G. Chen, J. Wu, Z. Wang, H. Zhu, S. Zhu, Q. Zhang, *Sci. Adv.* **2025**, *11*, eadv5292.
[45] J. Heckel, S. Loescher, R. T. Mathers, A. Walther, *Angew. Chem. Int. Ed.* **2021**, *60*, 7117–7125.
[46] S. Zhuo, C. Song, Q. Rong, T. Zhao, M. Liu, *Nat. Commun.* **2022**, *13*, 1743.
[47] D. Bruder, M. A. Graule, C. B. Teeple, R. J. Wood, *Sci. Rob.* **2023**, *8*, eadf9001.
[48] H. Ye, B. Wu, S. Sun, P. Wu, *Nat. Commun.* **2024**, *15*, 885.
[49] M. Elsayed, A. Isah, M. Hiba, A. Hassan, K. Al-Garadi, M. Mahmoud, A. El-Husseiny, A. E. Radwan, *J. Petrol. Explor. Prod. Technol.* **2022**, *12*, 2747–2784.
[50] Y. Liu, J. Zhang, P. Wu, *CCS Chem* **2025**, *7*, 484–492.
[51] S. Sun, P. Wu, *Chin. J. Polym. Sci.* **2017**, *35*, 700–712.